



Nickel separation from human blood samples based on amine and amide functionalized magnetic graphene oxide nano structure by dispersive sonication micro solid phase extraction

Anne Tréguët^a, Masoud Khaleghi Abbasabadi^b and Pooya Gholami^{c*}

^a Department of Chemistry, University Paris-Saclay, Saint-Aubin, Paris, France.

^b Department of Chemistry, Iran University of Science and Technology, Tehran, Iran

^c Nano Technology Center, Research Institute of Petroleum Industry (RIPI), P.O. Box 14665-1998, Tehran, Iran

ARTICLE INFO:

Received 18 Dec 2019

Revised form 6 Feb 2020

Accepted 27 Feb 2020

Available online 25 Mar 2020

Keywords:

Nickel,

Human blood,

Fe₃O₄-supported Amine

/Amide-functionalized graphene oxide,

Dispersive sonication micro solid phase extraction

ABSTRACT

Nickel (Ni) is toxic effect on human body and must be determined in human blood samples. In this study, Ni ions separated and preconcentrated from blood samples based on magnetic Fe₃O₄-supported amine/amide-functionalized graphene oxide (Fe₃O₄@A/A-GO) nanoparticles by dispersive sonication micro solid phase extraction (DS-μ-SPE). By procedure, 10 mg of Fe₃O₄@A/A-GO was dispersed in 10 mL of human blood samples with sonication for 5.0 min and then separated from liquid phase with magnetic accessory. The Ni ions was extracted based on amine/amide covalence bonding of Fe₃O₄@A/A-GO sorbent (Ni---: NH₂). Then, the Ni ions back-extracted from Fe₃O₄@A/A-GO in low pH with nitric acid (0.2 mL, 0.3 M) which was diluted with DW up to 0.5 mL and finally, was determined by ET-AAS (peak area). The LOD, linear range (LR), enrichment factor (EF) and absorption capacity (AC) were obtained 35 ng L⁻¹, 0.15 -7.2 μg L⁻¹, 19.8 and 131.6 mg g⁻¹, respectively. The method was validated by spiking samples.

1. Introduction

Nickel (Ni) is one of the toxic compounds in water contamination and caused to acute and chorionic effect in human bodies[1]. Ni(II) are released into environment from waste of different chemical factories such as battery manufacturing, mining and electroplating. The air of near factories contain the significant amount of heavy metals such as nickel and caused to adverse effects in environment

and humans[2]. Nickel is known to bind to specific proteins and/or amino acids in the blood serum and the placenta. Orally absorbed nickel is distributed to the kidneys, followed by the liver, brain, and heart. The harmful health effects of nickel lead to possible symptoms includes, chronic bronchitis, lung dysfunction, cancer in lung and nasal sinus[3]. Other target organs include the cardiovascular system, immune system, and the blood. In large doses (>0.5 g), some forms of nickel may be acutely toxic to humans when taken orally. Oral LD₅₀ values for rats range from 67-9000 mg Ni per kg (ATSDR).

*Corresponding Author: Pooya Gholami

Email: pooya1989gh@gmail.com

<https://doi.org/10.24200/amecj.v3.i01.96>

Toxic effects of oral exposure to nickel usually involve the kidneys with some evidence from animal studies showing a possible developmental/reproductive toxicity effect (ATSDR). Normal range for Ni in healthy peoples is $0.2 \mu\text{g L}^{-1}$ in serum and less than $3.0 \mu\text{g L}^{-1}$ in human urine. A national health and nutritional examination survey (NHNES) of hair found mean nickel levels of 0.39 mg L^{-1} , with 10% of the population having levels less than 1.5 mg L^{-1} [4,5]. The vary techniques was used for measurement of nickel (Ni^{2+}) in human bodies such as serum and blood samples. Due to previous studies, the flame atomic absorption spectrometry (F-AAS) and electrothermal atomic absorption spectrometry (ET-AAS) were reported for analysis of heavy metals such nickel (Ni) which was suitable for the determination in biological matrixes [6-9]. Occasionally, the atom trapping flame atomic absorption spectrometry (AT-FAAS) and fluorescence spectrometry (XRF) also was used for heavy metal determination such as nickel in biological samples [10, 11]. Also, different methods such as, polarography [12], inductively coupled plasma-optical emission spectrometry (ICP OES, inductively coupled plasma-mass spectrometry (ICP-MS) [13, 14], and spectrophotometry [15] were used for nickel analysis in human samples [16]. But as difficulty matrixes in human biological samples such as blood or serum, the sample preparation is required to separation nickel ions from liquid phases. The different sample preparation technology exist for nickel extraction from blood samples such as liquid-liquid extraction (LLE) [17], solid-phase extraction (SPE) and functionalized magnetic-SPE [18], dispersive solvent by liquid-liquid microextraction method (DLLME) [19], phase extraction based on cloud point (CPE) [20], dispersive solid phase microextraction (D-SPME) [21], ultrasound-assisted solid phase extraction (USA-SPE) [22]. Recently, the dispersive sorbent in the liquid phase was presented as micro SPE (D- μ -SPE) for separation/determination of nickel in water and

biological samples [23]. Some advantages such as high extraction efficiency, simple usability, fast and low time caused to select as a favorite technique for metal extraction. The sorbent characterizations are a main factor which was effected on heavy metal extraction by the D- μ -SPE procedure. The selective of favorite nanostructures improved recovery. The different nanosorbent such as, carbon nanotubes (CNTs), graphene / graphene oxide sheets (NG, NGO) and silica (MSN) were used for extraction of Ni in blood samples [24-26]. Between them, the NGO was reported as efficient sorbents for metal extraction due to their surface properties. In this study, a novel sorbent based on Fe_3O_4 -supported amine/amide-functionalized graphene oxide ($\text{Fe}_3\text{O}_4@A/A\text{-GO}$) was used for separation/speciation Ni(II) from human blood samples by dispersive sonication micro solid phase extraction (DS- μ -SPE) at pH=8.0. The method was developed in blood samples by ET-AAS.

2. Experimental

2.1. Instrumental

The graphite furnace atomic absorption spectrophotometer (GF-AAS, 932 GBC, Aus) was used for nickel determination in blood samples with the Avanta software. The linear range of $3.0\text{-}150 \mu\text{g L}^{-1}$ (peak Area, Abs=1.91) was selected for Ni in optimized light. The current and wavelength of HCL lamp was adjusted 3.0 mA and 228.8 nm, respectively. The auto-sampler of spectrophotometer (Pal 3000) was used for micro injection ($1\mu\text{L}$) of sample volumes to furnace tube after adjusted injector. The pH of the sample was digitally calculated by Metrohm pH meter (Swiss). Fourier transform infrared (FT-IR) spectra were recorded from KBr pellets using a Perkin Elmer Spectrum 65 FT-IR spectrophotometer. Powder X-ray diffraction (XRD) was conducted on a Panalytical X'Pert PRO X-ray diffractometer. Scanning electron microscopy (SEM) images were obtained using a Tescan Mira-3 Field Emission Gun Scanning Electron Microscope (SEM). Magnetic

property of the catalyst sample was measured with a vibrating sample magnetometer (VSM) model LBKFB, Meghnatis Daghigh Kavir Co, Iran, at room temperature

2.2. Reagents

Chemicals including natural flake graphite (325 mesh, 99.95%), were purchased from Merck chemical company and used as received. The standard stock solutions (1000 mg L^{-1}) of Ni (II), acetone, acetate, HNO_3 , NaOH, HCl and other reagents were purchased from Merck (Darmstadt, Germany). Ultra-pure deionized water (DW) purchased from Milli-Q plus water purification system (USA). The standard and experimental solutions of Ni^{2+} (0.1, 0.2, 0.5, 1.0, 3, 5.9 and $7.0 \mu\text{g L}^{-1}$) were prepared daily by appropriate dilution of the stock solutions with DW. The pH of samples were used with appropriate buffer solutions including sodium acetate for pH 3.5–5.6, sodium phosphate for pH of 5.8–8.0, and ammonium chloride for pH 8–10. All the laboratory glassware and plastic tubes were cleaned by 5% (v/v) HNO_3 for at least 12 h and then washed many times with DW and dried in oven prior to use. All reagents for synthesis of $\text{Fe}_3\text{O}_4@A/A\text{-GO}$ prepared by RIPI Company.

2.3. Synthesis of graphene oxide (GO)

Graphite black powder was oxidized to GO following the modified Hummers method in the several steps [27-29]. Fore pre oxidation of graphite powder, 250 mL of H_2SO_4 was added to 5 g of graphite powder and the resulting mixture was stirred for 24 h. After 24 h, 30 g of KMnO_4 was added to the mixture stirring for 72 h at 50°C . Next, a solution of 45 mL of H_2O_2 (30%) in 400 mL of deionized water was added to the mixture after which the brown color of the mixture turned into bright yellow. The GO dark solution was centrifuged and washed with deionized water and 10% HCl solution, and dried at 65°C .

2.4. Preparation of nanomagnetic Fe_3O_4 -supported Amine/Amide-functionalized graphene oxide ($\text{Fe}_3\text{O}_4@A/A\text{-GO}$)

2.4.1. Acyl-chlorination of graphene oxide

In the first step, thionyl chloride 60 mL was added GO (0.3 g) and stirred in at 70°C for 24 h. After acyl-chlorination reaction, the Acyl-chlorination of GO was washed with THF four times and the precipitated dried at 65°C [30].

2.4.1 Functionalization of graphene oxide with Ammonia

A total of 1 g of Ammonia was added to Acyl-chlorinated GO (0.3 g). Then, the mixture was refluxed for 72 h at 120°C under argon condition. Finally, the mixture reaction washed with DI water. A dark powder of Amine/Amide-functionalized graphene oxide was obtained [31].

2.4.2 Nano magnetization of Amine/Amide-functionalized graphene oxide

The Fe_3O_4 -supported Amine/Amide-functionalized graphene oxide ($\text{Fe}_3\text{O}_4@A/A\text{-GO}$) nanoparticles were synthesized by co-precipitation of $\text{FeCl}_2 \cdot 4\text{H}_2\text{O}$ and $\text{FeCl}_3 \cdot 6\text{H}_2\text{O}$, in the presence of Amine/Amide-grafted graphene oxide. First, a solution of $\text{FeCl}_2 \cdot 4\text{H}_2\text{O}$ and $\text{FeCl}_3 \cdot 6\text{H}_2\text{O}$ was prepared with a molar ratio of 2:1. The weight ratio of GO to FeCl_3 in the nano composite was 1 per 20 ($\text{mGO} : \text{mFeCl}_3 = 1:20$). Afterward, 10 mg of Amine/Amide-grafted graphene oxide in 15 mL of DI water was ultrasonicated for 20 min. 12.5 mL solution of $\text{FeCl}_2 \cdot 4\text{H}_2\text{O}$ (125 mg) and $\text{FeCl}_3 \cdot 6\text{H}_2\text{O}$ (200 mg) in deionized water (10 mL) was added to the reaction mixture at room temperature. In order to raise pH value to 11, an aqua solution of 30% ammonia was added in the reaction mixture at 70°C . Then, the reaction mixture was allowed to cool to room temperature and $\text{Fe}_3\text{O}_4@A/A\text{-GO}$ washed five times with DI H_2O dried at 70°C [32].

2.5 Analytical Procedure

In proposed procedure, 10 mL of blood and

standard solutions was prepared by buffer solution. The whole blood samples diluted with DW (1:1) before procedure. By DS- μ -SPE procedure, the pH of the standard solution containing 0.2 -7.0 $\mu\text{g L}^{-1}$ of nickel was adjusted up to 8 and then 0.01 g of $\text{Fe}_3\text{O}_4@A/A\text{-GO}$ as adsorbent was added to samples. The standard / blood samples was shaken for 5.0 min at room temperature and Ni ions physically adsorbed on surface of $\text{Fe}_3\text{O}_4@A/A\text{-GO}$ and chemically extracted by amine and amide covalence bonding at pH=8. Then, the $\text{Fe}_3\text{O}_4@A/A\text{-GO}$ separated from liquid phase by magnetic accessory. Finally, the Ni ions back-extraction with nitric acid (0.2 M) from $\text{Fe}_3\text{O}_4@A/A\text{-GO}$ and after dilution up to 0.5 mL with DW was determined by ET-AAS. In optimized conditions, the recovery of physically and chemically adsorption by $\text{Fe}_3\text{O}_4@A/A\text{-GO}$ was almost obtained 25.3% and 97.8%, respectively. The extraction efficiency of proposed method based on $\text{Fe}_3\text{O}_4@A/A\text{-GO}$ was calculated by equation 1. The C_A is the stock concentrations of nickel and C_B is the remain concentration of Ni(II)

after procedure ($n=10$, Eq. 1).

$$\text{Recovery of extraction} = (C_A - C_B) / C_A \times 100 \text{ (Eq.1)}$$

3. Results and Discussion

3.1. Characterization of the nano $\text{Fe}_3\text{O}_4@A/A\text{-GO}$

The Fe_3O_4 -supported Amine/Amide-functionalized graphene oxide nanomagnetic ($\text{Fe}_3\text{O}_4@A/A\text{-GO}$) was synthesized according to the synthetic route shown in Figure 1. Firstly, graphite was oxidized to GO by the modified Hummers method [27-29]. Afterward, the GO was amination and amidation with Ammonia by according to our previously reported procedure [30, 31]. Finally, the resulted Amine/Amide-functionalized graphene oxide ($\text{Fe}_3\text{O}_4@A/A\text{-GO}$) was nano-magnetized by co-precipitation of ferrous (Fe^{2+}) and ferric (Fe^{3+}) ions in the presence of A/A-GO to afford the target adsorbent $\text{Fe}_3\text{O}_4@A/A\text{-GO}$ [32].

Figure 2 shows the FT-IR spectra of GO and $\text{Fe}_3\text{O}_4@A/A\text{-GO}$. The broad peak in the range between 2600-3500 cm^{-1} in the IR spectra of these compounds is related to the (O-H stretching)

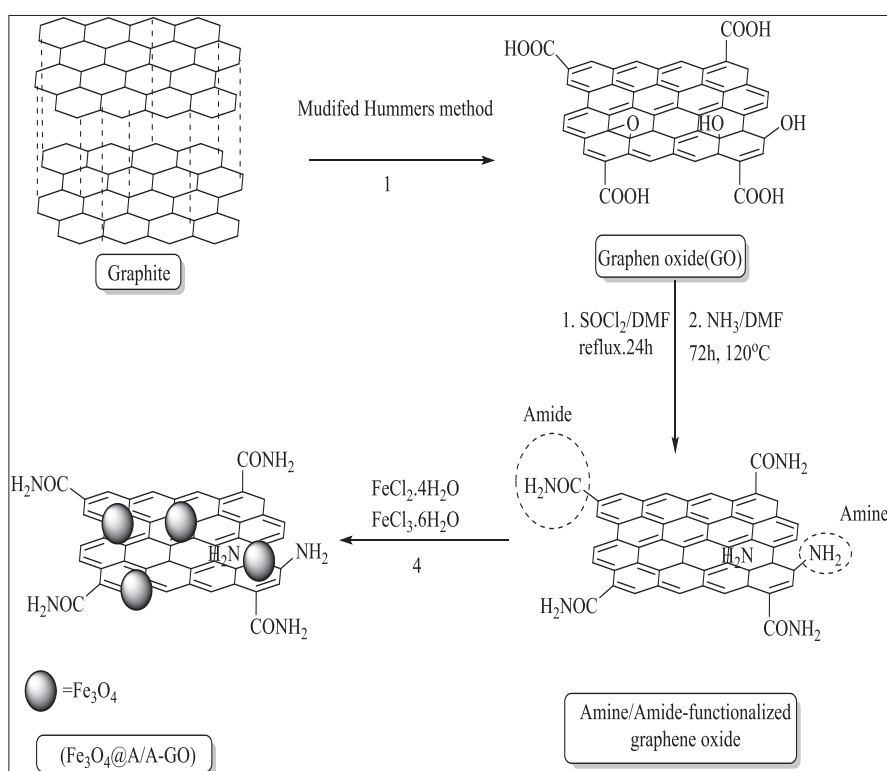


Fig 1. Synthetic route of $\text{Fe}_3\text{O}_4@A/A\text{-GO}$

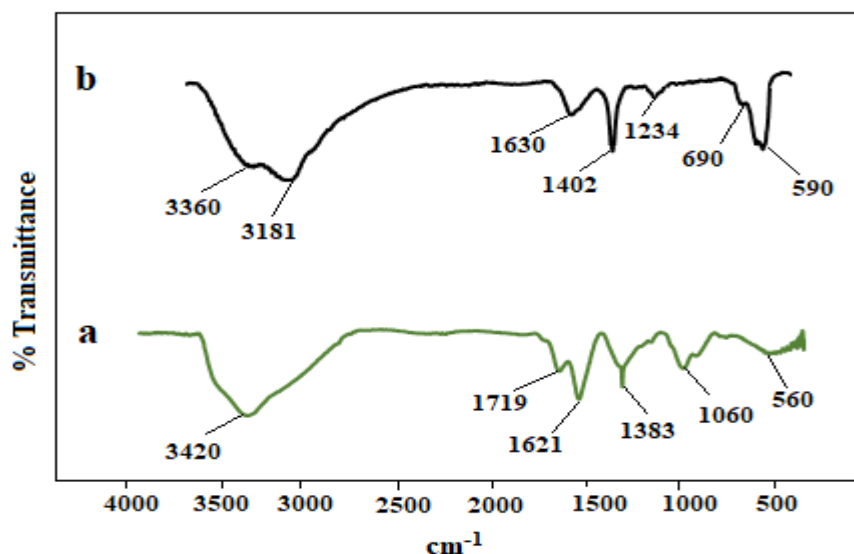


Fig. 2. FT-IR spectra of (a) GO, and (b) $\text{Fe}_3\text{O}_4@A/A\text{-GO}$

vibration of carboxylic and enolic functionalities [35]. The peaks at 3420, 1719, 1621, and 1060 cm^{-1} shown in the spectra of GO and $\text{Fe}_3\text{O}_4@A/A\text{-GO}$ are ascribed to the (C-O stretching), (C=C stretching), (C=O stretching), and (O-H stretching) respectively [33, 34]. Also, The absorption bands at 3360, 3181, 1630, and 1234 cm^{-1} shown in the spectra of GO and amination GO are ascribed to the stretching bands $\nu(\text{O-H})$, $\nu(\text{N-H})$, $\nu(\text{C=O})$, and $\nu(\text{C-N})$ respectively. In the spectrum of $\text{Fe}_3\text{O}_4@A/A\text{-GO}$, the peaks observed at around 628 and 583 cm^{-1} are related to the Fe-O stretching vibration [37-39]. These results prove that the successful Amination and amidation of GO and synthesis of

$\text{Fe}_3\text{O}_4@A/A\text{-GO}$.

The XRD patterns of GO, and $\text{Fe}_3\text{O}_4@A/A\text{-GO}$ are demonstrated in Figure 3 (a,b). GO has the two main peak at $2\theta = 11.5^\circ$, 42.58° are related to the diffraction planes of (002) and (100) respectively, which can be observed in the XRD patterns of both GO and $\text{Fe}_3\text{O}_4@A/A\text{-GO}$ [40-42]. As shown in Figure 3 (b), the peaks at $2\theta = 24^\circ$ and 42.58° It is evident from the XRD pattern of $\text{Fe}_3\text{O}_4@A/A\text{-GO}$ that was proved the presence of GO [42]. The main peaks at $2\theta = 30.12$, 35.45 , 43.07 , 56.97 , 62.47 in XRD pattern of $\text{Fe}_3\text{O}_4@A/A\text{-GO}$ are in good accordance with the standard XRD data of magnetite Fe_3O_4 . The main diffraction peaks at

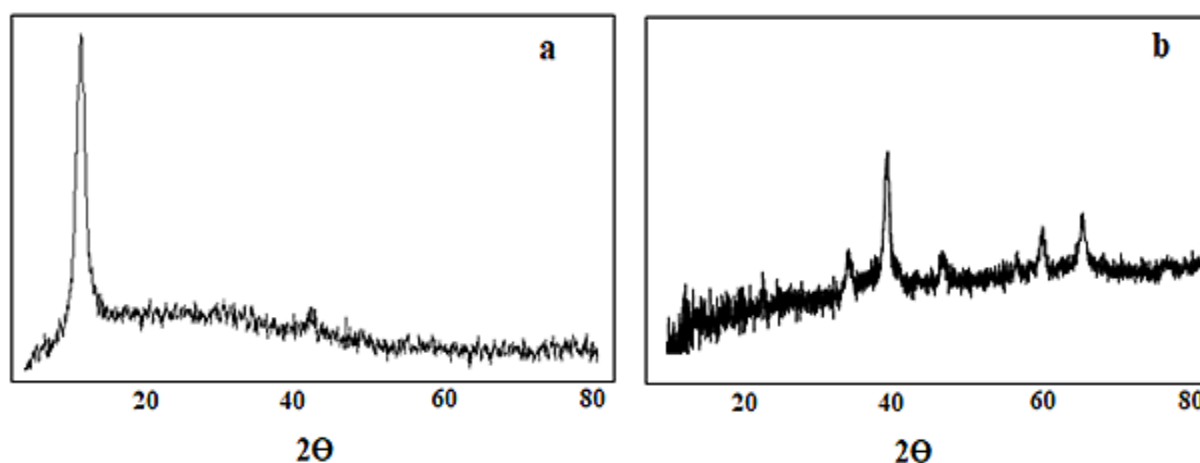


Fig. 3. XRD patterns of (a) GO, (b) $\text{Fe}_3\text{O}_4@A/A\text{-GO}$

$2\theta^\circ = 62.47, 56.97, 43.07, 35.45, 30.12$ are related to the reflection planes of cubic spinel crystal structure of Fe_3O_4 at (440), (511), (400), (311), (220) respectively [43-50].

The SEM image of GO shows that graphene oxide nano sheets consists of randomly accumulated and wrinkled thin sheets (Fig. 4a). Also, the SEM image of $\text{Fe}_3\text{O}_4@A/A\text{-GO}$ shows in Figure 4(b) that the average diameter of Fe_3O_4 nanoparticles was about 35.43 nm and indicate a regularly spherical morphology on A/A-GO [51-52].

The Magnetic behavior of the $\text{Fe}_3\text{O}_4@A/A\text{-GO}$ was recorded using a VSM. As shown in the Figure 5, the saturation magnetization of $\text{Fe}_3\text{O}_4@A/A\text{-GO}$ was found to be 42 emu g^{-1} . This amount of a saturation magnetization value, the magnetized nanocomposite is expected to have considerable

paramagnetism to make it magnetically separable from reaction mixture [32, 48].

3.2. Optimization of extraction procedure

For efficient extraction of nickel ions in human blood samples, the main parameters must be studied. The effective features such as, pH, sample volume, amount of $\text{Fe}_3\text{O}_4@A/A\text{-GO}$, shaking time and interferences ions must be optimized. Chemical bonding was strongly depended on the pH solutions. By procedure, the effect of pH on extraction of nickel through the amine functional group of $\text{Fe}_3\text{O}_4@A/A\text{-GO}$ was evaluated. For this purpose, the different pH values from 1 to 11 with nickel concentration of $0.2\text{-}7 \mu\text{g L}^{-1}$ as LLOQ and ULOQ was examined according to DS- μ -SPE procedure. Obviously, the maximum of extraction

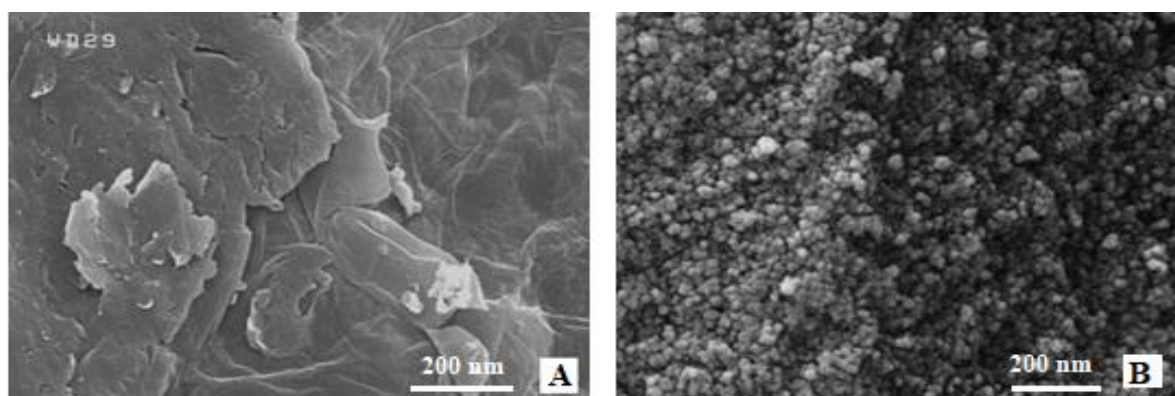


Fig. 4. SEM images of (a) GO, (b) $\text{Fe}_3\text{O}_4@A/A\text{-GO}$

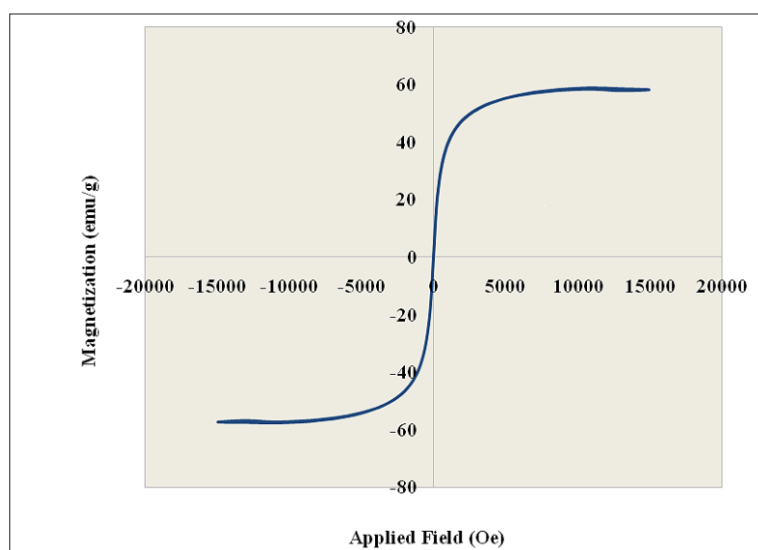


Fig. 5. VSM curve of $\text{Fe}_3\text{O}_4@A/A\text{-GO}$

efficiencies for Ni (II) ions based on Fe₃O₄@A/A-GO were obtained at pH range of 8.2, and then the recoveries were decreased by increasing or decreasing of pH (Fig. 6). In optimized conditions, the effect of sample volume of blood on nickel extraction was studied between 2-20 mL. The results showed, the optimum extraction was achieved for 12 mL of blood sample and 15 mL of standard samples, So, 10 mL of sample volume was used for further studies. Also, the amount of Fe₃O₄@A/A-GO for nickel extraction was evaluated by DS-μ-SPE procedure. Based on experimental results, 10 mg of Fe₃O₄@A/A-GO was selected as optimum point. The sonication time for extraction of Ni(II) was studied in optimized pH. Based on previous research, kind and size of adsorbents are the most important factors for extraction and sonication time. Therefore, the effect of sonication in blood samples was examined by DS-μ-SPE procedure. The results showed, the maximum efficiency was achieved at 5 min. The concentration of Interfering ions such

as Na⁺, K⁺, Mg²⁺, Ca²⁺, Cu²⁺, Zn²⁺, Co²⁺, Al³⁺, Hg²⁺, SO₃²⁻, I⁻, NO₃⁻, Cl⁻ and F⁻ caused less than ± 5% deviation in the recovery of Ni(II) as the tolerance limit. So, the interfering ions has no effect on the recovery efficiencies of Ni(II) in blood samples.

3.3. Validation methodology

Many methods was used for validation of methodology by SPE [53-55]. The analytical results of the developed DS-μ-SPE procedure were shown method at optimum conditions (Table 1). After sample preparation, Ni concentration in human blood and standard samples was determined by ET-AAS. The Human blood, serum and plasma as a real sample was used for determination of Ni by DS-μ-SPE procedure. The results was verified by analyzing the spiked samples with standard concentration of Ni (II) in human samples (Table 2). Based on results, a high and favorite recovery was obtained by spiking samples which confirms the accuracy of results in difficulty matrix. The

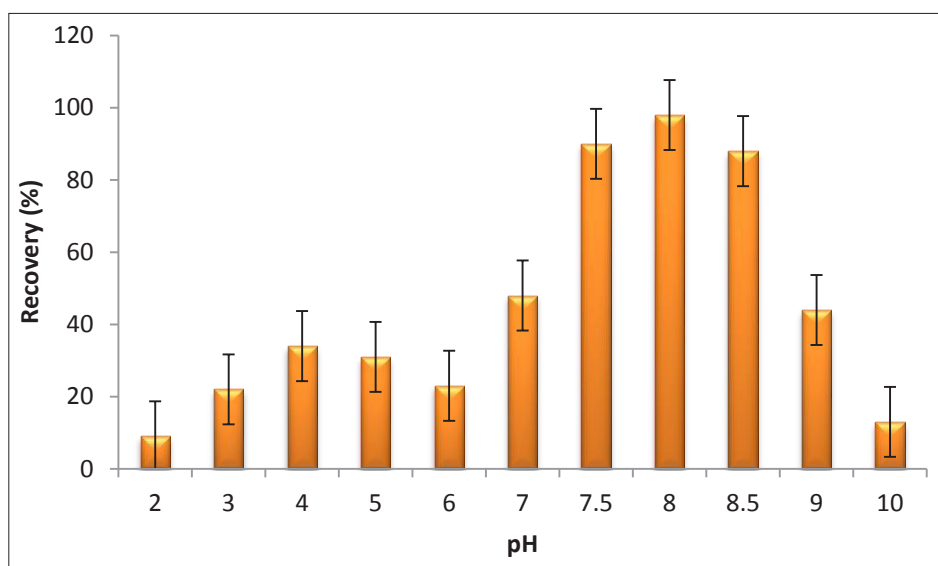


Fig. 6. The effect of pH on nickel extraction by DS-μ-SPE procedure

Table 1. Analytical results for Ni(II) extraction based on Fe₃O₄@A/A-GO by DS-μ-SPE

Element	^a SV	^b LR	^c R ²	^d LOD (n = 10)	^e RSD (%)	^f EF
Ni(II)	10	0.15- 7.2	0.9997	0.035	2.8%	19.8

^a sample volume (mL), ^b Linear rang ($\mu\text{g L}^{-1}$), ^cLimit of detection ($\mu\text{g L}^{-1}$), ^dRelative standard deviation, ^e enrichment factor(EF),

Table 2. Determination of nickel in blood, serum and plasma solutions by DS- μ -SPE procedure (mean intra –day and inter day for 10 samples)

Sample	Added($\mu\text{g L}^{-1}$)		* DS- μ -SPE ($\mu\text{g L}^{-1}$)		Recovery (%)
	Intra-day	Inter day	Intra-day	Inter day	
blood	-----	-----	3.65 ± 0.18	3.48 ± 0.15	-----
	3.0	-----	6.57 ± 0.28	-----	97.3
	-----	3.0	-----	6.51 ± 0.32	101.0
Plasma	-----	-----	1.45 ± 0.06	1.57 ± 0.07	-----
	1.5	-----	2.88 ± 0.13	-----	95.3
	-----	1.5	-----	2.99 ± 0.14	94.6
Serum	-----	-----	2.92 ± 0.14	2.86 ± 0.12	-----
	3.0	-----	6.02 ± 0.27	-----	103.3
	-----	3.0	-----	5.82 ± 0.25	98.6

*Mean of three determinations of samples \pm confidence interval (P = 0.95, n = 10)

recoveries of spiked samples demonstrated that the results was satisfactory for Ni analysis by DS- μ -SPE. In order to validate the method, the extraction efficiency for intra-day and inter day analysis was evaluated by spiking samples (Table 3).

4. Conclusions

A fast and efficient method based on $\text{Fe}_3\text{O}_4@A/A\text{-GO}$ as adsorbent was used for preconcentration, separation of trace Ni (II) in human blood samples by DS- μ -SPE procedure. The mechanism of extraction was achieved by interaction between negative charge (-) of amine group of $\text{Fe}_3\text{O}_4@A/A\text{-GO}$ with positive charge (+) of nickel ions in

favorite pH ($\text{Ni}^{2+} \dots \text{NH}_2$). After extraction, the concentration of nickel was determined by ET-AAS technique. Finally, the developed method has low ion interference, simple usage with low LOD, favorite RSD(%) values and good LR with high recoveries for Ni extraction in blood samples (>95%). Therefore, the proposed method can be considered as applied techniques for Ni separation and determination in blood samples by DS- μ -SPE coupled to ET-AAS.

5. Acknowledgements

The authors wish to thank the Research Institute of Petroleum Industry (RIPI) for financial support to

Table 3. Validation of methodology for Ni(II) extraction from human samples based on $\text{Fe}_3\text{O}_4@A/A\text{-GO}$ by DS- μ -SPE procedure

Sample*	Added ($\mu\text{g L}^{-1}$)	*Found ($\mu\text{g L}^{-1}$)	Recovery (%)
Blood A	---	2.61 ± 0.13	---
	2.5	5.07 ± 0.24	98.4
Blood B	---	1.73 ± 0.08	---
	2.0	3.76 ± 0.18	101.5
Serum C	---	3.06 ± 0.15	---
	3.0	5.98 ± 0.33	97.3
Serum D	---	2.72 ± 0.14	---
	3.0	5.68 ± 0.28	98.6
Plasma E	---	1.46 ± 0.11	---
	1.5	3.02 ± 0.16	104.6
Plasma F	---	0.25 ± 0.02	---
	0.25	0.49 ± 0.03	96.0

*Mean of three determinations of samples \pm confidence interval (P = 0.95, n = 10)

carry out this research.

6. References

- [1] A. Abbas, A.M. Al-Amer, T. Laoui, M.J. Al-Marri, M.S. Nasser, M. Khraisheh, Heavy metal removal from aqueous solution by advanced carbon nanotubes: critical review of adsorption applications, *Sep. Purif. Technol.*, 157 (2016) 141-61.
- [2] S. Feng, X. Wang, G. Wei, P. Peng, Y. Yang, Z. Cao, Leachates of municipal solid waste incineration bottom ash from Macao: Heavy metal concentrations and genotoxicity, *Chemosphere.*, 67 (2007) 1133-1137.
- [3] S.K. Seilkop, A.R. Oller, Respiratory cancer risks associated with low-level nickel exposure: An integrated assessment based on animal, epidemiological, and mechanistic data, *Regul. Toxicol. Pharm.*, 37 (2003) 173–190.
- [4] Agency for Toxic Substances and Disease Registry, Division of Toxicology and Human Health Sciences, 1600 Clifton Road NE, Mailstop S102-1, Atlanta, GA 30333, revision 2019.
- [5] Agency for Toxic Substances and Disease Registry (ATSDR), Toxicological profile for Nickel. Atlanta, GA: U.S. Department of Health and Human Services, Public Health Service, 2005.
- [6] N. Altunay, A. Elik, R. Gürkan, Vortex assisted-ionic liquid based dispersive liquid-liquid microextraction of low levels of nickel and cobalt in chocolate-based samples and their determination by F-AAS, *Microchem. J.*, 147 (2019) 277-285.
- [7] L. A. Escudero, A. J. Blanchet, L. L. Sombra, J. A. Salonia, J. A. Gasquez, Determination of the total and extractable fraction of Ni in lake sediments and natural waters of San Luis (Argentina) by F-AAS using a simple solid phase extraction system, *Microchem. J.*, 116 (2014) 92-97.
- [8] M. Felipe-Sotelo, A. Carlosena, J. M. Andrade, M. J. Cal-Prieto, D. Prada, Slurry-based procedures to determine chromium, nickel and vanadium in complex matrices by ET-AAS, *Microchem. J.*, 81 (2005) 217-224
- [9] A. Baysal, S. Akman, A rapid solid sampling method for determination of nickel and copper along human hair by ET-AAS, *Microchem. J.*, 98 (2011) 291-296.
- [10] G. Özzybek, B. Alacakoç, Trace determination of nickel in water samples by slotted quartz tube-flame atomic absorption spectrometry after dispersive assisted simultaneous complexation and extraction strategy, *Environ. Monit. Assess.*, 190 (2018) 498.
- [11] J. Shan Qun, W. Xiang Yu, S. Jin Lyu, Analysis of nickel distribution by synchrotron radiation X-ray fluorescence in nickel-induced early- and late-phase allergic contact dermatitis in Hartley guinea pigs, *Chinese Med. J.*, 132 (2019)1959-1964.
- [12] S. Kanchi, B. Ayyappa , M. Sabela , K. Bisetty, N Venkatasubba Naidu, Polarographic Interaction of Nickel (II) with Ammonium Piperidine-1-Carbodithioate: Application to Environmental Samples, *J. Environ. Anal. Chem.*, 1 (2014) 107.
- [13] Y. Min Park, J. Yeon Choi, E. Yeong Nho, C. Mi Lee, Determination of macro and trace elements in canned marine products by inductively coupled plasma optical emission spectrometry (ICP-OES) and ICP-mass spectrometry (ICP-MS), *J. Anal. Lett.*, 52 (2019) 1018-1030.
- [14] S. C. Wilschefski, M. R. Baxter, Inductively coupled plasma mass spectrometry: introduction to analytical aspects, *Clin. Biochem. Rev.*, 40 (2019) 115-133.
- [15] A. Fadhil Khudhair, M. Khudhair Hassan , H. F. Alesary , A. S. Abbas, Simple pre-concentration method for the determination of nickel(II) in urine samples using UV-VIS spectrophotometry and flame atomic absorption spectrometry techniques, *Indones. J. Chem.*, 19 (2019) 638 – 649.
- [16] G. Saravanabhavan, K. Werry, M. Walker, D. Haines, M. Malowany, C. Khoury, Human biomonitoring reference values for metals and trace elements in blood and urine derived from the Canadian Health Measures Survey 2007–2013, *Int. J. Hyg. Environ. Health*, 220 (2017) 189–200.
- [17] S. M. Sorouraddin, M. A. Farajzadeh H. Nasiri, Picoline based-homogeneous liquid–liquid microextraction of cobalt(ii) and nickel(ii) at trace levels from a high volume of an aqueous sample, *Anal. Methods*, 11 (2019) 1379-1386.
- [18] S.Z. Mohammadi, H. Hamidian, L. Karimzadeh,

- Z. Moeinadini, Simultaneous extraction of trace amounts of cobalt, nickel and copper ions using magnetic iron oxide nanoparticles without chelating agent, *J. Anal. Chem.*, 68 (2013) 953–958.
- [19] A. Hol, A. Akdogan, A.A. Kartal, U. Divrikli, L. Elci, Dispersive liquid-liquid microextraction of nickel prior to its determination by micro sample injection system-flame atomic absorption spectrometry, *Anal. Lett.*, 47 (2014) 2195–2208.
- [20] Q. Han, Y. Huo, L. Yang, X. Yang, Y. He, J. Wu, Determination of trace nickel in water samples by graphite furnace atomic absorption spectrometry after mixed micelle-mediated cloud point extraction, *Molecul.*, 23 (2018) 2597.
- [21] S. Davari, F. Hosseini, H. Shirkhanloo, Dispersive solid phase microextraction based on amine-functionalized bimodal mesoporous silica nanoparticles for separation and determination of calcium ions in chronic kidney disease, *Anal. Methods Environ. Chem.*, J. 1 (2018) 57-66.
- [22] H. Shirkhanloo, Z. Karamzadeh, J. Rakhshshah, N. Motakef Kazemi, A novel biostructure sorbent based on CysSB/MetSB@MWCNTs for separation of nickel and cobalt in biological samples by ultrasound assisted-dispersive ionic liquid-suspension solid phase micro extraction, *J. Pharm. Biomed. Anal.*, 172 (2019) 285-294.
- [23] M. Behbahani, A. Veisi, F. Omid, A. Noghrehabadi, A. Esrafil, M. Hossein Ebrahimi, Application of a dispersive micro-solid-phase extraction method for pre-concentration and ultra-trace determination of cadmium ions in water and biological samples, *Appl. Organometal. Chem.*, (2017) e4134.
- [24] M. A. Habila, Z. A. AlOthman, E. Yilmaz, M. Soylak, Activated carbon cloth filled pipette tip for solid phase extraction of nickel (II), lead (II), cadmium (II), copper(II) and cobalt (II) as 1,3,4-thiadiazole-2,5-dithiol chelates for ultra-trace detection by FAAS, *Int. J. Environ. Anal. Chem.*, 98 (2018) 171-181.
- [25] M.R. Pourjavid, M. Arabieh, A. A. Sehat, Study on column SPE with synthesized graphene oxide and FAAS for determination of trace amount of Co(II) and Ni(II) ions in real samples, *Mater. Sci. Eng. C*, 47 (2014) 114-122
- [26] S. N. Nabavi, S. M. Sajjadi, Z. Lotfi, Novel magnetic nanoparticles ($\text{CoO-Fe}_2\text{O}_3\text{@SiO}_2\text{@TiO}_2$) as adsorbent in ultrasound-assisted micro-solid-phase extraction for rapid pre-concentration of some trace heavy metal ions in environmental water samples: desirability function, *Chem. Papers*, 74 (2019)1143–1159.
- [27] W.S.J. Hummers, R.E. Offeman, Preparation of Graphitic Oxide, *J. Am. Chem. Soc.*, 80 (1958) 1339-1339.
- [28] M.K. Abbasabadi, A. Rashidi, S. Khodabakhshi, Benzenesulfonic acid-grafted graphene as a new and green nanoadsorbent in hydrogen sulfide removal, *J. Nat. Gas Sci. Eng.*, 28 (2016) 87-94.
- [29] M. Khaleghi-Abbasabadi, D. Azarifar, Magnetic Fe_3O_4 -supported sulfonic acid-functionalized graphene oxide ($\text{Fe}_3\text{O}_4\text{@GO-naphthalene-SO}_3\text{H}$): a novel and recyclable nanocatalyst for green one-pot synthesis of 5-oxo-dihydropyrano[3,2-c]chromenes and 2-amino-3-cyano-1,4,5,6-tetrahydropyrano[3,2-c]quinolin-5-ones, *Res. Chem. Intermed.*, 45 (2019) 2095–2118.
- [30] M. Khaleghi Abbasabadi, A. Rashidi, J. Safaei-Ghomi, S. Khodabakhshi, R. Rahighi, J. A new strategy for hydrogen sulfide removal by amido-functionalized reduced graphene oxide as a novel metal-free and highly efficient nanoadsorbent, *Sulfur Chem.*, 36 (2015) 660-671.
- [31] K.S. Novoselov, Z. Jiang, Y. Zhang, S.V. Morozov, H.L. Stormer, U. Zeitler, J.C. Maan, S. Boebinger, P. Kim, A.K. Geim, Room-temperature quantum hall effect in graphene, *Sci.*, 315 (2007) 1379.
- [32] M.Z. Kassaee, E. Motamedi, M. Majdi, Magnetic Fe_3O_4 -graphene oxide/polystyrene: Fabrication and characterization of a promising nanocomposite, *Chem. Eng. J.*, 172 (2011) 540-549.
- [33] S. Khodabakhshi, F. Marahel, A. Rashidi, M. Khaleghi Abbasabadi, A Green Synthesis of Substituted Coumarins Using Nano Graphene Oxide as Recyclable Catalyst, *J. Chin. Chem. Soc.*, 62 (2015) 389-392.
- [34] D. Azarifar, M. Khaleghi-Abbasabadi, Fe_3O_4 -supported N-pyridin-4-amine-grafted graphene oxide as efficient and magnetically separable novel nanocatalyst for green synthesis of 4H-chromenes

and dihydropyrano[2,3-c]pyrazole derivatives in water, *Chem. Intermed.*, 45 (2019) 199–222.

- [35] C. Nethravathi, M. Rajamathi, Chemically modified graphene sheets produced by the solvothermal reduction of colloidal dispersions of graphite oxide, *Carbon*, 46 (2008) 1994–1998.
- [36] D. Chen, H. Zhang, K. Yang, H. Wang, Functionalization of 4-aminothiophenol and 3-aminopropyltriethoxysilane with graphene oxide for potential dye and copper removal, *J. Hazard. Mater.*, 310 (2016) 179–187.
- [37] J.S. Wang, R.T. Peng, J.H. Yang, Y.C. Liu, X.J. Hu, Preparation of ethylenediamine-modified magnetic chitosan complex for adsorption of uranyl ions *Carbohydr. Polym.*, 84 (2011) 1169–1175.
- [38] X.J. Hu, Y.G. Liu, H. Wang, A.W. Chen, G.M. Zeng, S.M. Liu, Removal of Cu(II) ions from aqueous solution using sulfonated magnetic graphene oxide composite, *Sep. Purif. Technol.*, 108 (2013) 189–195.
- [39] L.Z. Bai, D.L. Zhao, Y. Xu, J.M. Zhang, Y.L. Gao, L.Y. Zhao, J.T. Tang, Inductive heating property of graphene oxide–Fe₃O₄ nanoparticles hybrid in an AC magnetic field for localized hyperthermia, *Mater. Lett.*, 68 (2012) 399–401.
- [40] M. Khaleghi Abbasabadi, A. Rashidi, J. Safaei-Ghomi, S. Khodabakhshi, R. Rahighi, A new strategy for hydrogen sulfide removal by amido-functionalized reduced graphene oxide as a novel metal-free and highly efficient nano-adsorbent, *J. Sulfur Chem.*, 36 (2015) 660–671.
- [41] S. Khodabakhshi, B. Karami, Graphene oxide nanosheets as metal-free catalysts in the three-component reactions based on aryl glyoxals to generate novel pyranocoumarins, *New J. Chem.*, 38 (2014) 3586–3590.
- [42] H. Kim, K.Y. Park, J. Hong, K. Kang, All-graphene-battery: bridging the gap between supercapacitors and lithium ion batteries, *Sci. Rep.*, 4 (2014) 5278.
- [43] C. Hou, Q. Zhang, M. Zhu, Y. Li, H. Wang, One-step synthesis of magnetically-functionalized reduced graphite sheets and their use in hydrogels, *Carbon*, 49 (2011) 47–53.
- [44] E. Rafiee, M. Khodayari, Two new magnetic nanocomposites of graphene and 12-tungstophosphoric acid: characterization and comparison of the catalytic properties in the green synthesis of 1,8-dioxo-octahydroxanthenes, *RSC Adv.*, 16 (2016) 36433–36440.
- [45] S. Khodabakhshi, M. Khaleghi Abbasabadi, S. Heydarian, S. Gharehzadeh Shirazi, F. Marahel, Fe₃O₄ Nanoparticles as Highly Efficient and Recyclable Catalyst for the Synthesis of 4-Hydroxy-3-[aryloyl(benzamido)methyl]coumarin under Solvent-Free Conditions, *Lett. Organ. Chem.*, 12 (2015) 465–470.
- [46] J. Wang, Z. D. Han, The combustion behavior of polyacrylate ester/graphite oxide composites, *Polym. Adv. Technol.*, 17 (2006) 335–340
- [47] P. J. Yen and C. C. Ting, et al., Facile production of graphene nanosheets comprising nitrogen-doping through in situ cathodic plasma formation during electrochemical exfoliation, *J. Mater. Chem. C*, 5 (2017) 2597–2602
- [48] C. C. Yang and M. H. Tsai, et al., Carbon Nanotube/Nitrogen-Doped Reduced Graphene Oxide Nanocomposites and Their Application in Supercapacitors, *J. Nanosci. Nanotechnol.*, 17 (2017) 5366–5373.
- [49] L. J. Li and C. W. Chu, et al., Plasma-assisted electrochemical exfoliation of graphite for rapid production of graphene sheets, *RSC Adv.*, 4(2014)6946–6949.
- [50] M. Rohaniyan, A. Davoodnia, A. Nakhaei, Another application of (NH₄)₄₂[Mo^{VI}₇₂Mo^V₆₀O₃₇₂(CH₃COO)₃₀(H₂O)₇₂] as a highly efficient recyclable catalyst for the synthesis of dihydropyrano[3,2]chromenes, *Appl. Organometal. Chem.*, 30 (2016) 626–629
- [51] J. Wang and Z. D. Han, The combustion behavior of polyacrylate ester graphite oxide composites, *Polym. Adv. Technol.*, 17(2006) 335–340.
- [52] X. Wang and L. Zhang, Green and facile production of high-quality graphene from graphite by the combination of hydroxyl radicals and electrical exfoliation in different electrolyte systems, *RSC Adv.*, 9 (2019) 3693–3703.
- [53] ZH Mousavi, A Rouhollahi, Preconcentration and determination of heavy metals in water, sediment and biological samples, *J. Serb. Chem. Soc.*, 76 (2011) 1583–1595

- [54] HZ Mousavi, A Asghari, Determination of Hg in water and wastewater samples by CV-AAS following on-line preconcentration with silver trap, *J. Anal. Chem.*, 65 (2010) 935-939.
- [55] A Khaligh, F Golbabaie, Z Sadeghi, A Vahid, A Rashidi, On-line micro column preconcentration system based on amino bimodal mesoporous silica nanoparticles as a novel adsorbent for removal and speciation of chromium (III, VI) in environment samples, *J. Environ. Health Sci. Eng.*, 13 (2015) 47.